2012 MRS
FALL MEETING

First Principles Calculations and Experiments for Cu-Mg/Li Hydrides Negative Electrodes

SCHOLARONE™
Manuscripts

First principles calculations and experiments for Cu-Mg/Li hydrides negative electrodes

M.H. Braga[1,a], V. Stockhausen[1], M. Wolverton[2], J.A. Ferreira[3], J.C.E. Oliveira[1,b]

[1]Engineering Physics Department, FEUP, Porto University, R. Dr. Roberto Frias, s/n, 4200-465, Porto, Portugal and CEMUC[a] and CFP[b].

[2]LANSCE, Lujan Center, Los Alamos National Laboratory, mail stop: H805, NM, 87545, USA.

[3]Energy and Geology National Laboratory, LNEG, R. da Amieira, S. Mamede Infesta, Portugal.

ABSTRACT

We have studied $CuLi_{0.08}Mg_{1.92}$ and determined that the compound reacts with hydrogen to form $CuLi_{0.08}Mg_{1.92}H_5$ [1]. Additionally, we have proposed the compound as a negative electrode material which is the main purpose of the present study. Moreover, we have observed that the latter compound acts as a catalyst in the formation of MgH_2, LiH, TiH_2 [2] and hydrogen desorption. In this work, first principles and phonon calculations were performed in order to establish the reactions occurring at the negative electrode of a Li conversion battery in presence of $CuLi_{0.08}Mg_{1.92}H_5$ and (Li) – solid solution of Mg in Li – approximately Li_2Mg_3. We have calculated the minimum theoretical specific capacity to be 1156 mAh/g (for an anode with 100% of $CuLi_{0.08}Mg_{1.92}H_5$) and the $\Delta E_{eq} = 0.81$ V (vs. Li^+/Li) at 298 K. Furthermore, we have determined all the reactions occurring in the referred system and its sequence using Inelastic Incoherent Neutron Scattering (IINS) and X-Ray Diffraction (XRD).

INTRODUCTION

Li-ion batteries are appealing as they provide higher energy density compared to other rechargeable batteries. The use of Li-metal as negative electrode improves the specific capacity but rises safety issues. In a Nat. Mater. paper, Oumellal et al. [3] investigated the use of MgH_2, TiH_2 and $NiMg_2H_4$ as enhanced negative electrodes in Li batteries. These authors addressed a type of reaction with implications for both Li-ion batteries and fuel cells. It was shown that MgH_2 reacts with Li according to the equation $MgH_2+2Li^++2e^-<->Mg+2LiH$ ($\Delta E_{eq} = 0.56$ V Li^+/Li). MgH_2 electrodes lead to a theoretical maximum discharge capacity of 2034 mAh/g (experimental: 1500 mAh/g), while they possess a reversible capacity of 1125 mAh/g in comparison with 372 mAh/g for graphite (currently used in commercial Li-ion batteries). Although Oumellal et al. succeeded in reducing cell polarization, metal hydride electrodes remain plagued by a large initial irreversible capacity (~30%) and poor capacity retention limited to less than 20-50 cycles regardless of the cycling rate or voltage window. Other Li alloy anodes, like $Li_{22}Si_5$, also suffer from short life-cycle due to the extremely high increase in volume ($\Delta V_{theoretical} = 316$ %).

We have studied $CuLi_{0.08}Mg_{1.92}$ and determined that the compound reacts with hydrogen to form $CuLi_{0.08}Mg_{1.92}H_5$[1]. Moreover, we have observed that the latter compound acts as a catalyst in the formation/hydrogen desorption of MgH_2, LiH and TiH_2 [2]. Therefore, such a system is a potential candidate for application as negative electrode in Li conversion batteries according to

what was proposed by Oumellal et al. [3]. Furthermore, due to higher electron conductivity, $CuLi_{0.08}Mg_{1.92}H_5$ negative electrode will most likely not need to be enclosed into copper foam - lowering the specific capacity of the negative electrode - as MgH_2 did; and a nanostructured negative electrode is not compulsory since $CuLi_{0.08}Mg_{1.92}$ absorbs hydrogen at a much lower temperature than MgH_2 and with enhanced kinetics.

EXPERIMENT AND CALCULATIONS

An alloy of the system Cu-Li-Mg was prepared by melting the elements together, Cu (electrolytic, 99.99% purity, 325 mesh), Mg (99.8% purity, 200 mesh, Alfa Aesar), and small (less than 3mm wide) pieces of Li (99% purity, Alfa Aesar), at 1100 °C/1373 K for 1h using a stirring device. The resulting sample had 26.6 wt% of $CuLi_{0.08}Mg_{1.92}$, 64.1 wt% of (Li) ~ Li_2Mg_3 and 9.3 wt% of Cu_2Mg. Samples were first characterized by means of XRD using a Rigaku Ultima III powder diffractometer, and their composition was roughly determined by means of the Match software [4], which uses the "Reference Intensity Ratio method" RiR - method) [5] to obtain phase fractions. Patterns were collected with $CuK\alpha$ typically from $2\theta = 15$ to $70°$ with steps of $0.02°$ and a counting time of 10 s per bin.

The latter sample was then sealed inside a stainless steel crucible and kept at 200 °C (473 K) for 24 h under H_2 at P = 60 bar. After the latter procedure, a part of the sample was sealed in an aluminum can and introduced into the neutron scattering instrument and quenched to 10 K in FDS. This temperature took 2-3 h to be achieved. The other part of the sample was submitted to XRD in the mentioned powder diffractometer. The previous measurement conditions were used.

The Filter Difference Spectrometer (FDS) is used for vibrational spectroscopy by inelastic incoherent neutron scattering. We have analyzed, at 10 K, the mentioned sample from the Cu-Li-Mg-H system and its parent sample from the Cu-Li-Mg system (to get the background).

Density Functional Theory (DFT) calculations with Projector Augmented Wave (PAW) pseudopotentials [6], as implemented in the Vienna *Ab initio* Simulation Package (VASP) code [7], were performed. A plane wave cutoff of 400 eV, and k-mesh of 4x4x4 were used. Calculations were done in real space and were performed within the P1 space group supercells containing 144 atoms for $CuLi_{0.08}Mg_{1.92}$ and 129 atoms for $CuLi_{0.08}Mg_{1.92}H_5$. The supercells contained as many atoms as possible to allow better approximations with the real Li concentrations (but not such to make the calculation time completely impractical). We have furthermore optimized the MgH_2, $CuMg_2$, Cu_2Mg, LiH, and Li_2Mg_3 compounds, H_2 molecule "in a box" and Li and Mg crystal structures to be able to calculate the Gibbs energy of all the reactions at different temperatures. More accurate parameters apply for these last compounds since primitive cells were used. For the H_2 molecule, a cubic box of 10^3 Å was used with a plane wave cutoff of 700 eV, and k-mesh of 8x8x8 as it is usually used in the literature to obtain accurate formation and reaction enthalpies, specifically when dealing with H_2 (e.g. [8-10]). The Generalized Gradient Approximation (GGA), and the Perdew–Burke–Ernzerhof (PBE) functional [11] were used and no magnetic moments were included in the model.

The Phonon direct method [12] was engaged to predict the lattice dynamics using the harmonic approximation on the VASP minimized structures that had the lowest ground state energy.

DISCUSSION

XRD measurements highlight a sequence of events that constitute an autocatalytic cycle within a system initially constituted by three phases $CuLi_{0.08}Mg_{1.92}$ + (Li) + Cu_2Mg (Figure 1). Upon hydrogen uptake at 200ºC (473 K), the first hydride phase to be formed is $CuLi_{0.08}Mg_{1.82}H_5$ [13] which is in agreement with our calculations in Table I, (I) and (III). XRD experiments highlight as well the initial presence of (Li) ~ Li_2Mg_3 that is a body centered cubic structure, bcc-A2, as pure Li. After hydrogenation, the latter phase cannot be seen anymore and γ-MgH_2, Mg (hexagonal) and LiH become detectable by XRD.
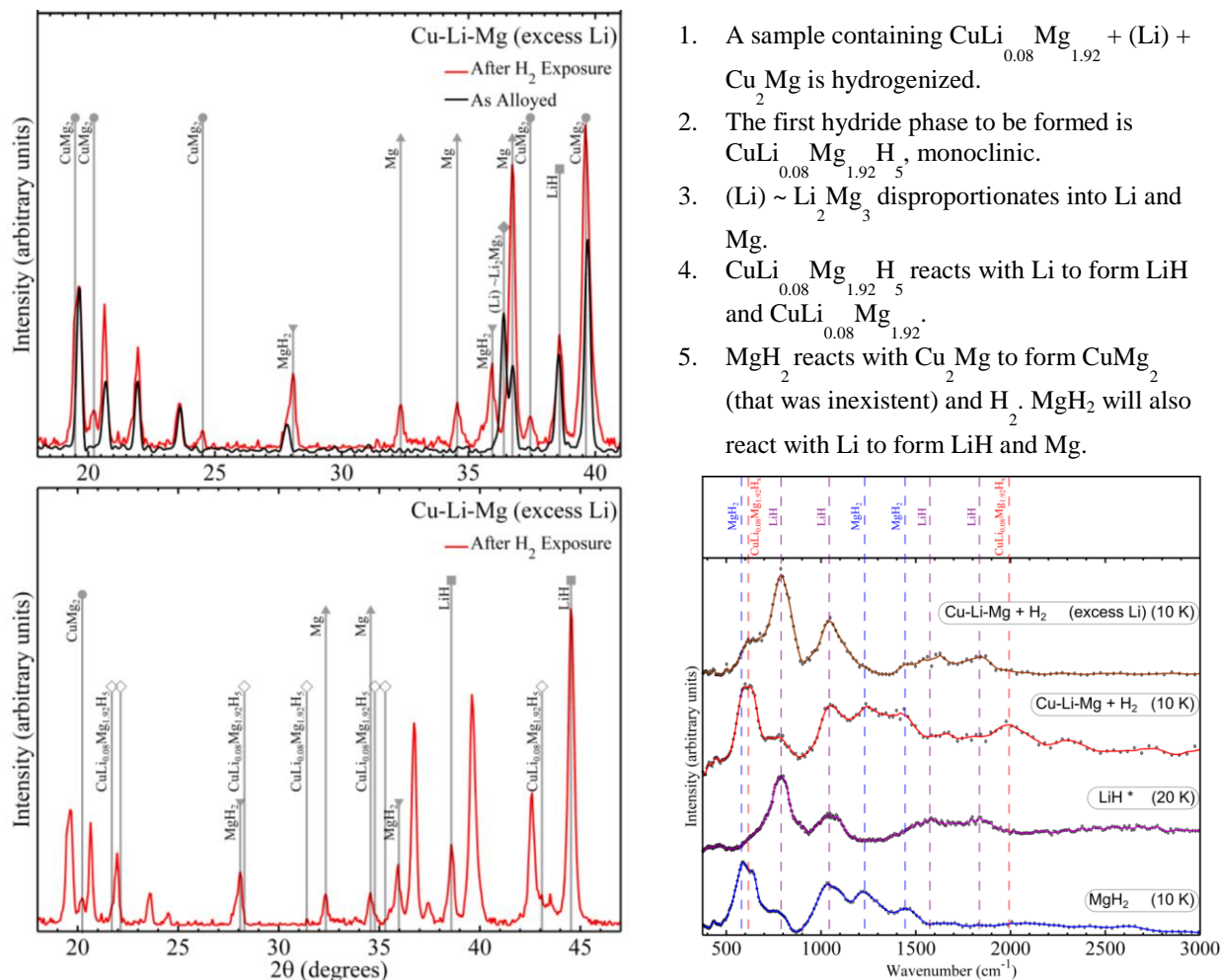
1. A sample containing $CuLi_{0.08}Mg_{1.92}$ + (Li) + Cu_2Mg is hydrogenized.
2. The first hydride phase to be formed is $CuLi_{0.08}Mg_{1.92}H_5$, monoclinic.
3. (Li) ~ Li_2Mg_3 disproportionates into Li and Mg.
4. $CuLi_{0.08}Mg_{1.92}H_5$ reacts with Li to form LiH and $CuLi_{0.08}Mg_{1.92}$.
5. MgH_2 reacts with Cu_2Mg to form $CuMg_2$ (that was inexistent) and H_2. MgH_2 will also react with Li to form LiH and Mg.

Figure 1. Diffraction patterns (left) and inelastic spectra (right) of a sample containing 26.6 wt% (6.0 at%) of $CuLi_{0.08}Mg_{1.92}$, 64.1 wt% (92.5 at%) of (Li) ~ Li_2Mg_3 and 9.3 wt% (1.5 at %) of Cu_2Mg. On the upper left, the parent and the hydrogenated sample's diffraction patterns can be compared. On the bottom right, the formation of LiH, Mg and MgH_2 is very unambiguous. It is possible that $CuLi_{0.08}Mg_{1.92}H_5$ is also present in the IINS spectrum as it is pointed out.

According to our previous experiments and calculations (Table I), after (III) - which is the first reaction to occur-, (V) occurs due to the presence of $CuLi_{0.08}Mg_{1.92}H_5$ and Li after the

disproportionation of (Li) into Li and Mg. The presence of MgH_2 and Li will also propitiate reaction (IV) in Table I. The magnesium hydride, MgH_2, in its tetragonal gamma crystal structure, P4/mnm, is present either by direct hydrogenation of Mg, upon (Li) disproportionation, or after $CuLi_{0.08}Mg_{1.82}H_5$ disproportionation into $CuLi_{0.08}Mg_{1.42}H_4 + (1/2) MgH_2$. The latter process will be thoroughly discussed and published later on. Finally, it can also be inferred from XRD measurements and confirmed with calculations (Table I, reverse (II)) that $CuMg_2$ and H_2 will be formed, due to the presence of both Cu_2Mg and MgH_2. In Figure 1, it can be observed that $CuMg_2$ will only be present after hydrogenation; it did not exist in the parent phase.

From IINS measurements (Figure 1), it is clearly detected the presence of LiH after hydrogenation at 200 ºC (473 K) followed by quenching to 10 K. MgH_2 is also present and so is $CuLi_{0.08}Mg_{1.82}H_5$. It is important to highlight that IINS is particularly sensible to hydrogen's vibration modes and consequently to hydrides, since hydrogen's incoherent cross-section is particularly high.

All the reactions occurring in this autocatalytic system can be completely proved by both experimental (Figure 1 and 2, [1,13]) and first principles calculations data (Table I). It is an extremely interesting and well identified process. In Figure 2 it can be moreover observed that a sample containing $CuLi_{0.08}Mg_{1.92}H_5$, Cu_2Mg and MgH_2 can desorb hydrogen at temperatures and pressures that are within the "applicable" range.

One of the applications for this system is addressed by the work of Oumellal et al. [3]. The latter group worked with hydrides as negative electrodes. It occurred to us that a negative electrode made out of $CuLi_{0.08}Mg_{1.82}H_5$, instead of MgH_2, or eventually of a chemical mixture of $CuLi_{0.08}Mg_{1.82}H_5 + (Li)$ would be advantageous. An enhancement would be avoiding the polarization owed to the presence of hydrogen and its diffusion properties [3].

Table I. Thermodynamic values for selected reactions occurring in the Cu-Li-Mg-H system, calculated using first principles implemented at VASP and Phonon.

	Reaction	T (K)	ΔH (kJ/mol H_2)	ΔS (kJ/mol H_2)	ΔG (kJ/mol H_2)
(I)	$(2/5)CuLi_{0.08}Mg_{1.92} + H_2 \rightarrow$ $(2/5)CuLi_{0.08}Mg_{1.92}H_5$	298	-23.4	-0.121	12.7
		450	-25.3	-0.125	31.2
					T_{dec} = 193 K = -80 °C
(II)	$(2/3)CuMg_2 + H_2 \rightarrow (1/3)Cu_2Mg + MgH_2$	298	-69.9	-0.128	-31.8
		450	-71.4	-0.129	-13.3
					T_{dec} = 553 K = 280 °C
(III)	$(¼)CuLi_{0.08}Mg_{1.92} + (¼)CuMg_2 + H_2 \rightarrow$ $(¼)CuLi_{0.08}Mg_{1.92}H_5 + (1/8)Cu_2Mg + (3/8)MgH_2$	298	-46.6	-0.125	-9.52
		450	-48.3	-0.127	8.9
					T_{dec} = 376 K = 103 °C

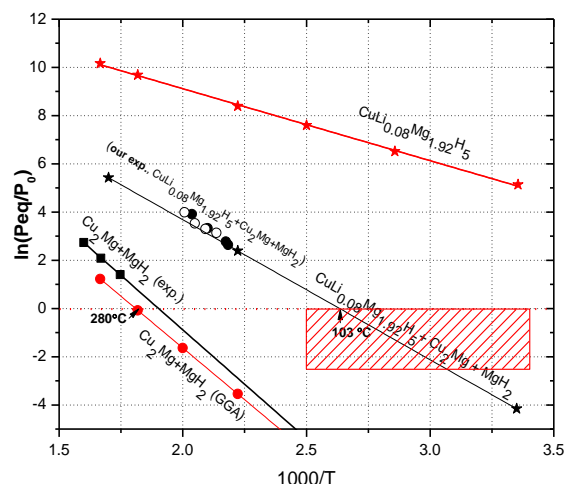|	Reaction	T (K)	ΔH (kJ/mol Li)	ΔS (kJ/mol Li)	ΔG (kJ/mol Li)
(IV)	$MgH_2 + 2Li \rightarrow 2LiH + Mg$		-54.4	-0.009	-51.8
		298			
					E_{eq} = 0.54 V (Li$^+$/Li)
(V)	$CuLi_{0.08}Mg_{1.92}H_5 + 5Li \rightarrow$ $5LiH_2 + CuLi_{0.08}Mg_{1.92}$	298	-85.4	-0.023	-78.0
					E_{eq} = 0.81 V (Li$^+$/Li)

Figure 2. Van't Hoff plot for several products resulting from sample hydrogenation of samples of the Cu-Li-Mg system. Details of the experimental procedures taken to obtain the data marked with (exp.) – filled and unfilled black circles and filled diamonds - may be found in [1]. The patterned rectangle highlights the range of temperatures and pressures with practical applications. Straight lines were calculated with thermodynamic values shown in Table I.

A further advantage of $CuLi_{0.08}Mg_{1.82}H_5$ is the fact that this material is semiconductor (band gap energy, E_g = 1.8 eV similarly to $NiMg_2H_4$, 1.7 eV [14]) and not insulator as MgH_2, E_g = 5.5 eV [15], which makes a negative electrode of this compound enhanced in terms of electrical conductivity. On the other hand, a sample with $CuLi_{0.08}Mg_{1.82}$ + (Li) – chemically mixed - will be straightly forward obtained by melting stoichiometric amounts of the reagents after taking into account the phase diagram of the Cu-Li-Mg system [16]. Moreover, $CuLi_{0.08}Mg_{1.82}$ does not have to be reduced to nano sizes to form $CuLi_{0.08}Mg_{1.82}H_5$ at practical temperatures and increased kinetics. To enhance conductivity and life cycle, Oumellal et al. [3] used MgH_2 nanopowders embedded in copper foam. The latter procedure has the disadvantage of decreasing the specific capacity of the electrode.

$CuLi_{0.08}Mg_{1.82}H_5$ shows a ΔE_{eq} = 0.81 V (Li^+/Li) at 298 K and a theoretical specific capacity of 1156 mAh/g (for an anode with 100% of $CuLi_{0.08}Mg_{1.92}H_5$) (Figure 3, Table I (V)).
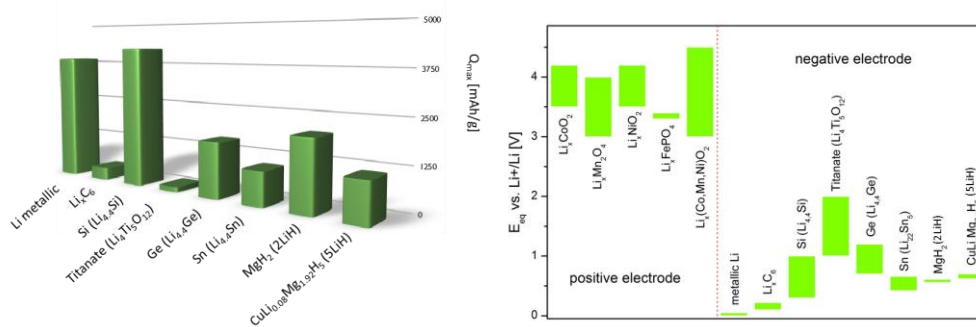

Figure 3. On the left side the comparison between the specific capacities of different negative electrodes. We point the graphite (currently used in commercial Li-ion batteries) with a theoretical specific capacity of 372 mAh/g (Li_xC_6). On the right side, several theoretical voltages, for different negative electrodes can be compared with those for positive electrodes. Data for MgH_2 and $CuLi_{0.08}Mg_{1.82}H_5$ were calculated using our results in Table I.

CONCLUSIONS

The advantages of $CuLi_{0.08}Mg_{1.92}H_5$ as a negative electrode are:

1. It shows a specific capacity which is close to that of pure MgH_2 and can be enhanced if a sample of $CuLi_{0.08}Mg_{1.92}H_5$ + (Li) is used;
2. $CuLi_{0.08}Mg_{1.92}$ and (Li) coexist in thermodynamic equilibrium and therefore these two phases can be found in close contact within the electrode;
3. The electrode will probably not need extra Cu foam to improve electrical conductivity since the material has higher electrical conductivity than MgH_2. The nano sized compounds made out of $CuLi_{0.08}Mg_{1.92}H_5$, are yet to be explored and so is its microstructure.

ACKNOWLEDGMENTS

REFERENCES

1. M.H. Braga, J.A. Ferreira and M. Wolverton, J. Therm. Anal. Calorim. 108 (2), 733 (2012).
2. M.H. Braga, M.J. Wolverton, A. Llobet and L.L. Daemen, Mater. Res. Soc. Symp. Proc. 1262-W03-05 (2010).
3. Y. Oumellal, A. Rougier, G.A. Nazri, J.-M. Tarascon, L. Aymard, Nat. Mater. 7, 916 (2008).
4. Match, http://www.crystalimpact.com/ (2012).
5. P.M. de Wolff and J.W. Visser in Absolute Intensities. Report 641.109. Technisch Physische Dienst, Delft, Netherlands. Reprinted in Powder Diffract 3, 202 (1988).
6. P.E. Blochl, Phys. Rev. B 50, 17953 (1994).
7. G. Kresse and J. Furthmüller, Phys. Rev. B 54 (16), 11169 (1996).
8. M.J. van Setten, G.A. de Wijs, G. Brocks, Phys. Rev. B 76, 075125 (2007).
9. L.G. Hector Jr, J.F. Herbst, J. Phys. Cond. Matt. 20, 064229 (2008).
10. H. Nenonen, The role of van der Walls interactions in the case of H_2 absorption on ruthenium (0001) surface. Master's thesis, Lappeenranta University of Technology, 2012, p. 19.
11. J.P. Perdew and Y. Wang, Phys. Rev. B 45, 13244 (1992).
12. K. Parlinski, Z.Q. Li and Y. Kawazoe, Rev. Lett. 78, 4063 (1997).
13. M.H. Braga, A. Acatrinei, M. Hartl, S. Vogel, Th. Proffen, L. Daemen, J. Phys. Conf. Ser., 251, 012040, (2010).
14. D. Lupu, R. Sarbu, A. Biris, Int. J. Hydrog. Energy 12, 425 (1987).
15. J. Isidorsson, I.A. Giebels, H. Arwin, R. Griessen, Phys. Rev. B 68, 115112 (2003).
16. M.H. Braga, L.F. Malheiros, M. Hämäläinen, Thermochim. Acta, 344, 47 (2000).